nature portfolio

Peer Review File

Lipid synthesis, triggered by PPARγ T166 dephosphorylation, sustains reparative function of macrophages during tissue repair

REVIEWER COMMENTS

Reviewer #1 (Remarks to the Author):

The study by Zuo et al. investigates the role of PPARg-regulated lipid synthesis program in the reparative function of macrophages during skin wound repair. Through scRNAseq of different wound repair models in mice, the authors have identified the lipid synthesis pathway to be enriched in macrophages from the repairing stage. Analyses of potential transcription factor binding sites led to the conclusions that PPARg might be a master regulator of macrophage reparative function through the control of de novo lipogenesis and that inhibition of PPARg T166 phosphorylation increases its activity to regulate lipogenesis and promote wound healing. Mechanistically, the authors suggest that fatty acids, products of de novo lipogenesis, not only activate STAT3 to upregulate wound repairing factors (e.g., Vegfb, Pdgfb and Tgfb1) but also support ER expansion for protein synthesis and secretion.

The study started out with seemingly unbiased approaches with various seq and omics studies. However, the authors have never disclosed the complete set of data analyses. Instead, what the readers have been given were data that supported the proposed mechanism. In addition, most of the experimental details have not been provided, making the data interpretation difficult.

Specific comments:
1. The premise of the entire study is based on the scRNAseq analyses in Fig. 1. However, the authors failed to provide sufficient information that describes: (1) the 9 different models; (2) the RNAseq analyses of these models; (3) the definition of phase I/II in each model; (4) the statistical analyses applied to determine "high and low" in Fig. 1E; (5) what are the genes in "FAO" and "FAS"; and (6) how do they come up with the 9 genes examined in Fig. 1D. Without these key pieces of information, one could not determine whether FAS is the most relevant pathway in the so-called reparative function of macrophages.
2. Similarly, the actual data and detailed experimental conditions for lipidomics, ChIPseq and CUT&RUN analyses were missing. The authors also did not provide a strong justification for studying IL-10 as an upstream signal. Of note, mouse genetic studies have clearly demonstrated that IL-10 is not required for the wound healing and tissue repair processes (e.g., J of Surgical Research 285:26). These prior studies do not support the authors' hypothesis and conclusion.
3. The authors stated that de novo-synthesized fatty acids could act as ligands for STAT3. In Fig. 6D-G, they showed that free fatty acids induce STAT3 phosphorylation. What were the FFAs and concentrations used? Fatty acids exist in the forms of fatty acyl-coA or triglycerides inside the cells. It's unclear how FFA could reach STAT3? In Fig. 6, the authors need to show that any effects of FFAs are abolished in STAT3 KO macrophages. In addition, what's o and p (and their concentrations) in Fig. 6G?
4. In Fig. 7, the CDDO treatment should be repeated to include PPARgKO and PPARa/a models to show the specificity.
5. The following information should be provided: (1) p7, the source of public transcriptomes of M(IL10); (2) Fasn KO, PPARKO and PPARa/a macrophages and/or mice; (3) how many genes used for SCENIC analysis in Fig. 3A, etc.

Reviewer #2 (Remarks to the Author):

This is a very nice manuscript looking at the role of PPARg and associated lipid activated STAT3 on macrophage function in several injury models, namely wound repair. It is mechanistic and well written; however I have the following comments that I think will strengthen the findings and broaden the conclusions.
1. For Figure 1, how were monocyte-macrophages defined? Further, what time points post injury were the harvests obtained -- phase 2 is rather broad and many would suggest that days 3-5 is still a transitional period, hence examining early/middle/late may allow for seeing the transition of macrophages.
2. For Fig 2/3, RNA seq of the actual wound macrophages - isolated at an early/late time point

would yield more relevant information than sequencing BMDMs and would be more representative of the plasticity that exists within the wound tissues.
3. For Fig 4 in the PPAR overexpressers, these assays need to be analyzed in wound macrophages in order to truly represent the changes in the tissue - BMDMs do not accurately depict the tissue changes.
4. The acute wound healing model used does not accurately represent how human wounds heal - would need splinted/casted model to prevent contraction healing and show these changes in wound repair are relevant to human disease.

Reviewer #3 (Remarks to the Author):

General impression
Macrophages remain an important immune cell player during the wound healing process. Yet, much less is known about the molecular mechanisms governing macrophage metabolic and phenotypic plasticity in driving wound reparation. The manuscript describes a molecular mechanism involving PPARγ-mediated metabolic reprogramming that facilitates the maturation of reparative macrophages during wound healing. Through a series of in vitro and in vivo experiments, it was revealed that T166 dephosphorylation of PPARγ during the recovery stage promotes lipogenesis in macrophages for the expansion of endoplasmic reticulum, subsequently increasing the secretion of STAT3-induced growth factors like Tgfb1, Vegfb and Pdgfb to promote wound closure. Furthermore, Zuo et al. demonstrated the clinical translatability of this work using topical application of CDDO which inhibits PPARγ T166 phosphorylation. The following points highlight my concerns:

Major comments

1. The title should be revised to "PPARγ T166 dephosphorylation…" to reflect the exact regulatory mechanism.
2. In Figure 1 and S1A-C, it is unclear how the macrophages from scRNAseq of different tissues were classified into phase I (acute injury stage) and phase II (reparative stage). Acute injuries in different types of tissues are likely to have different rates of recovery. For instance, dermal injuries tend to heal faster compared to spinal cord or muscle injuries. Therefore, the criteria to distinguish the acute and reparative phases in all tissue injuries should be outlined. Further, some models were of different types of sequencing experiments (e.g. single cell nature, bulk, or macrophage isolated only). How did the authors reconcile the differences?
3. In Figure 1C, it is unclear what the "Gene number" 34, and 8 numbers mean. The authors should indicate with much greater clarity on the meaning and derivations of the terms gene number, and the quantities of 34 and 8.
4. The authors should indicate what the values stated in Figure 1E, meant. In the legend, it is stated high, low but not what values these represent. This comment applies to other figures of similar nature.
5. It is unclear which model Figure 1F is referring to. Is it a pseudotime analysis? Although the main text (line 127) alludes to Figure 1F representing the skin macrophages, but the UMAP visualized in Figure 1F is vastly different from that of Figure 1B.
6. In Figure 1F, the method to annotate different subtypes of macrophages in phase I and II, i.e. M0, M(IFNg), M(LPS), M(IL4) and M(IL10), is not elaborated. Any particular reason why M(IFNg) is missing in Figure 1G? Ideally, the colors for different macrophage subpopulations in Figure 1F and G should be consistent to avoid confusion.
7. While Figure 1C & E are derived from scRNAseq of different tissues, validation of the role of reparative macrophages was primarily conducted using skin injury in mice models and scratch tests using dermal fibroblasts. Hence, it is cautious not to over-generalize the findings beyond the dermal injury context, especially in the discussion and conclusion.
8. The visualization of Figure 1G and 3E is confusing. It is unclear what the values represent. The error bars are also erroneous. What statistical test is used for the comparisons?
9. Figure S6A reveals possible accumulation of lipid droplets (white circular structures) in the dermis layers.

10. Did the SCENIC analysis also predict increased activity of STAT3 in reparative wound macrophages?
11. In Figure 6F-G, it is better to show fold change instead of change in CT values to avoid confusion.
12. In Page 16, Lines 328-329, it is important to demonstrate that the increased lipogenic products from phospholipid synthesis are directed to endoplasmic reticulum expansion. Tracing with [U-13C] glucose followed by endoplasmic reticulum isolation could potentially provide valuable insight. Furthermore, the data suggests a correlation between ER expansion and secretion of reparative proteins in reparative macrophages. To ascertain a causal relationship, the levels of reparative signals when ER expansion is inhibited should be examined.
13. The GEO accession numbers of RNAseq, CHIP-seq and CUT&RUN-seq should be provided.
14. Apart from being a PPARγ T166 phosphorylation inhibitor, bardoxolone (CDDO) is also a strong inducer of Nrf2 (PMID 34052830). Therefore, additional control groups/evaluations are needed to validate that the benefits are not confounded by Nrf2 signaling.

Minor comments
15. Error in Line 139 – Figure 2G should be Figure 1G.
16. For Figure 1G, authors should indicate what datasets were used and how the analyses were done.
17. Figure 3H, typo on x-axis, Bodioy should be Bodipy.
18. For Figure S5B, it is unclear how the genes were ranked. Are the gene ranked by comparing PPARg+/+ against PPARgA/A or the inverse?
19. In Page 9 Line 176, it should be "… the pro-migratory ability of dermal fibroblasts M(IL10) …".
20. In Fig. S4E, quantification of the fluorescence intensities and statistical analysis should be shown.
21. In Page 10 Line 205, it should be "…through dephosphorylating T166 site…".

Reviewer #4 (Remarks to the Author):

My review concentrates on the reproducibility of the bioinformatics analysis outlined in this manuscript, with a particular attention at the high-throughput technologies discussed.

Major:
1) The paper mentions that RNA-seq, ChIP-seq, and CUT&RUN-seq data are currently being uploaded to the Gene Expression Omnibus (GEO) database, emphasizing data availability. Authors are required to specify the superseries of the data in the manuscript and provide access tokens to reviewers.
2) Single cell data analysis. In the manuscript it is presented the reanalysis of 9 single cell datasets. The description provided in Material and Methods is not sufficient. It is required to authors to provide a github describing the full analysis performed on the datasets.
3) Github must also include the analysis performed with SCENIC software.
4) In the section RNA sequencing and data analysis, the thresholds, i.e. adj-pvalue and absolute log2FoldChange, used to identify the differentially expressed genes are not indicated.
5) The MACS2 analysis results must be also provided in Zenodo or figshare repository.
6) Bed files generated by the analysis of CUT&RUN-seq must also be provided in Zenodo or figshare repository.
7) The code used to generate Fig.1 B, E, F, G, Fig. 3 A, B, E and Fig. 5 A panels must be provided in the github.

Dear Editor,

Thank you for your invaluable assistance with our original manuscript (Submission ID: NCOMMS-24-00526-T) entitled "PPARγ T166 phosphorylation-mediated lipid synthesis sustains the reparative function of macrophages during tissue repair". We sincerely appreciate your interest in our work, diligent efforts in handling our paper, and valuable suggestions. Additionally, we are grateful for the thoughtful and constructive comments and suggestions provided by the reviewers. We have thoroughly addressed all major concerns raised by the reviewers and believe that these modifications strengthen our conclusion. The point-by-point responses are as follows:

Reviewer #1:

The study by Zuo et al. investigates the role of PPARg-regulated lipid synthesis program in the reparative function of macrophages during skin wound repair. Through scRNAseq of different wound repair models in mice, the authors have identified the lipid synthesis pathway to be enriched in macrophages from the repairing stage. Analyses of potential transcription factor binding sites led to the conclusions that PPARg might be a master regulator of macrophage reparative function through the control of de novo lipogenesis and that inhibition of PPARg T166 phosphorylation increases its activity to regulate lipogenesis and promote wound healing. Mechanistically, the authors suggest that fatty acids, products of de novo lipogenesis, not only activate STAT3 to upregulate wound repairing factors (e.g., Vegfb, Pdgfb and Tgfb1) but also support ER expansion for protein synthesis and secretion.

The study started out with seemingly unbiased approaches with various seq and omics studies. However, the authors have never disclosed the complete set of data analyses. Instead, what the readers have been given were data that supported the proposed mechanism. In addition, most of the experimental details have not been provided, making the data interpretation difficult.

Response: We greatly appreciate the thorough review and valuable suggestions you provided for our manuscript. We deeply apologize for any inconvenience caused by the absence of information and experimental details. In the revised manuscript, we have thoroughly addressed these concerns and believe that the provided details adequately support our findings.

Specific comments:

1. The premise of the entire study is based on the scRNAseq analyses in Fig. 1. However, the authors failed to provide sufficient information that describes: (1) the 9 different models; (2) the RNAseq analyses of these models; (3) the definition of phase I/II in each model; (4) the statistical analyses applied to determine "high and low" in Fig. 1E; (5) what are the genes in "FAO" and "FAS"; and (6) how do they come up with the 9 genes examined in Fig. 1D. Without these key pieces of information, one could not determine whether FAS is the most relevant pathway in the so-called reparative function of macrophages.

Response: Thank you for bringing that to our attention. In response, we have included additional information regarding scRNA-seq analyses in the revised manuscript. We believe that these details adequately support our findings. The point-by-point responses are as follows:

(1) The 9 different models: A comprehensive analysis of reparative macrophages across diverse tissues will enhance our understanding of the mechanisms underlying how metabolism influences macrophage reparative function. Thus, we obtained scRNA-seq datasets containing wound macrophages from 9 classic mouse wound healing models. The following table (Reviewer Only Table 1) will help you better understand the information about these 9 models. A table containing more detailed information has been submitted along with the revised manuscript as Supplementary Table 2. The manuscript has been annotated with yellow highlights to indicate corrections (Page 33 line 684-692).

Reviewer Only Table 1 scRNA-seq datasets used in this study.

Database	Dataset ID	Phase I	Phase II	Tissue	Study description
GEO	GSE141259	10 d	28 d	Lung	Bleomycin-mediated acute lung injury
GEO	GSE152501	1 d	7 d	Airway	Polidocanol-mediated airway injury
GEO	GSE163465	3 d	14 d	Heart	Left anterior descending coronary artery ligation
GEO	GSE180420	3 d	14 d	Kidney	Short ischemic reperfusion
GEO	GSE186986	1 d	5 d	Skin	Full-thickness excisional skin injury
GEO	GSE200843	1 d	7 d	Joint	Noninvasive single dynamic tibial compressive overload
GEO	GSE205037	3 d	7 d	Spinal cord	Laminectomy
GEO	GSE205690	4 d	7 d	Skeletal muscle	$BaCl_2$-induced skeletal muscle injury
Zenodo	6035873	2 d	4-7 d	Liver	Acetaminophen-induced acute liver damage

(2) The RNAseq analyses of these models: We have provided detailed information in the method part to help you better understand the data analysis procedures. The corrections have been marked by yellow highlight (Page 33 line 684-694, Page 34 line 705, Page 34-35 line 709-719, Page 35 line 723-724). Besides, the R scripts used for data analysis have been submitted to GitHub.

(3) The definition of phase I/II in each model: This is a crucial step in our scRNA-seq analysis. Experientially, in a full-thickness excisional skin injury model, the inflammatory phase (phase I) would occur 1-3 days post injury (dpi), while the reparative phase (phase II) would occur 5-7 dpi. However, as mentioned by reviewer #3 question 2, injuries in different types of tissues are likely to have different recovery rates. Besides, we observed that different injury methods can also result in varying rates of recovery within the same tissue. Thus, the definition of phase I/II should not be solely based on timepoints. Although the recovery rates vary across different tissues, similar biological processes occur following injury. When tissues are injured due to toxic or mechanical damage, an inflammatory response is induced by damage-associated molecular patterns and other pro-inflammatory molecules. This response is characterized by the recruitment, proliferation, and activation of diverse hematopoietic and non-hematopoietic cells such as neutrophils, macrophages, natural killer cells, and fibroblasts. When the wound-healing response is well organized and controlled, the number of pro-inflammatory cells decreases, and tissue function is restored [1]. Therefore, the microenvironment and tissue function changes can serve as ideal criteria for distinguishing inflammatory and reparative phases. These pieces of evidence were primarily derived from the source articles related to these datasets. We have provided some evidence at the end of the

letter for you and other reviewers to verify the definition of phases (Reviewer Only Table 3). A table containing PubMed ID for reviewers and readers to access the source articles has been submitted along with the revised manuscript as Supplementary Table 2. The corrections have been marked by yellow highlight in the revised manuscript (Page 33 line 692-694).

Typically, we chose the most appropriate timepoint for each phase to conduct the scRNA-seq analysis. However, for liver phase II, we were unable to isolate enough macrophages at a single timepoint for data analysis. We observed that both 4 and 7 dpi exhibited reparative phenotypes. Therefore, we selected both 4 and 7 dpi to represent this stage.

(4) The statistical analyses applied to determine "high and low" in Fig. 1E: Sorry for the lack of clarity regarding this legend. The "high and low" in Fig. 1e is the labels of heatmap legend that have no statistical meanings. This style of legend is commonly used in high-throughput analysis [2-4]. To avoid confusion, we have made modifications in the revised manuscript by replacing it with a standard legend (Fig. 1e). We believe that these changes will help you and readers easily understand the intended meaning conveyed by this plot.

(5) What are the genes in "FAO" and "FAS": The terms "Fatty acid biosynthesis" and "Fatty acid degradation" from the KEGG database were utilized to assess the metabolic activity of FAO and FAS in this study. These KEGG terms are widely used in metabolic analysis [5]. The corresponding KEGG IDs were annotated in the method part of the original manuscript, and it has also been included in the figure legend of the revised manuscript. The corrections have been marked by yellow highlight (Page 56 line 1167-1169).

(6) How do they come up with the 9 genes examined in Fig. 1D: The 9 genes examined in Figure 1D are the encoding genes of rate-limiting enzymes, transcription factors and functional proteins related to lipid metabolism. The following table (Reviewer Only Table 2) may help you have a better understanding of the function of these genes. We have checked the manuscript and realized that we did not provide a clear explanation of the function of these genes. We apologize for this oversight. To provide a clear representation for both you and the readers, we decided to include only the key genes involved in lipid anabolism (*Acaca*, *Acly* (Newly examined), *Fasn*, *Slc25a1*) and catabolism (*Cpt1a*, *Pnpla2*) in Fig. 1d and provide annotations for their gene functions below.

Reviewer Only Table 2 Genes used in Figure 1D.

Gene	Product type	Metabolic process	Product function
Fasn	Rate-limiting enzyme	Lipid anabolism	Catalyzing the synthesis of palmitate from acetyl-CoA and malonyl-CoA
Acaca	Rate-limiting enzyme	Lipid anabolism	Acetyl-CoA carboxylase activity
Pnpla2	Rate-limiting enzyme	Lipid catabolism	Triglyceride lipase activity
Cebpa	Transcription factor	Lipid anabolism	Promoting fatty acid biosynthesis and desaturation
Cpt1a	Rate-limiting enzyme	Lipid catabolism	Carnitine O-palmitoyltransferase activity and palmitoleoyltransferase activity
Dgat1	Rate-limiting enzyme	Lipid anabolism	Catalyzing the conversion of diacylglycerol to triacylglycerol
Plin2	Functional protein	Lipid storage	Lipid storage and long-chain fatty acid transport
Fabp4	Functional protein	Lipid transportation	Long-chain fatty acid transport
Slc25a1	Functional protein	Lipid anabolism	Export of citrate from the mitochondria into the cytoplasm

2. Similarly, the actual data and detailed experimental conditions for lipidomics, ChIPseq and CUT&RUN analyses were missing. The authors also did not provide a strong justification for

studying IL-10 as an upstream signal. Of note, mouse genetic studies have clearly demonstrated that IL-10 is not required for the wound healing and tissue repair processes (e.g., J of Surgical Research 285:26). These prior studies do not support the authors' hypothesis and conclusion.

Response: We are sorry for these oversights and have included additional information for lipidomics, ChIP-seq and CUT&RUN analyses in the method part of the revised manuscript. The corrections have been marked by yellow highlight (Page 37 line 760-761, Page 37 line 769, 777, Page 38 line 780-781, 786, Page 39 line 799, Page 39 line 806-810, Page 40-41 line 834-847, Page 41 line 855-860). Basically, the cell culture and experimental conditions were described in the sections titled "*Cell culture experiments*", "*BMDMs generation and in vitro treatment*" of method part, while the procedures to perform lipidomics, ChIP-seq and CUT&RUN analyses and data analyses were described in corresponding sections. The GEO accession for ChIP-seq and CUT&RUN data has been added to the revised manuscript (Page 47 line 969-976). lipidomics data are provided in Supplementary Table 3.

As for the utilization of IL-10. To the best of our knowledge, IL-10 induces a classical reparative phenotype of macrophages *in vitro* [1, 6]. M(IL10) has been extensively employed as a tool for investigating the reparative function of macrophages. Previous studies have demonstrated that M(IL10) exhibit enhanced efficacy in promoting wound healing following injury [7, 8]. Our data also revealed that the skin wound macrophages exhibited an M(IL10)-like phenotype during the reparative phase of wound healing (Fig. 1f). Therefore, IL-10 treated macrophage is an ideal model to investigate the mechanism of wound healing *in vitro*. Furthermore, we have included both M(IL10) and *in vivo* wound macrophages to support most of our hypothesis and conclusion, except for the experiments that require numerous cells as input, such as lipidomics, ^{13}C tracing, and ChIP-seq.

Indeed, we did not focus on the necessity of IL-10 signaling in wound healing. But we would like to stress out the complexity of *in vivo* activation of macrophages during wound healing. In the early stage of wound healing, macrophages will be activated under the stimulation of damage associated molecular patterns (DAMPs), pathogen-associated molecular patterns (PAMPs), growth factors, cytokines, and other mediators released in the local tissue microenvironment to promote inflammatory response [1]. When the wound healing is controlled, macrophages undergo a phenotypic transition towards a reparative state upon exposure to IL-4, IL-10, IL-13, IL-21, lipids, immune complexes, HDL, and other pro-resolving molecules [1, 9]. In this situation, inhibiting a single cytokine may not significantly impact the reparative phenotype of macrophages, as the other signal molecules may compensate for the absence of IL-10 in order to facilitate the reparative program of macrophages and sustain the progression of healing. Collectively, we believe that it is suitable to use IL-10 for *in vitro* experiments in this study.

3. The authors stated that de novo-synthesized fatty acids could act as ligands for STAT3. In Fig. 6D-G, they showed that free fatty acids induce STAT3 phosphorylation. What were the FFAs and concentrations used? Fatty acids exist in the forms of fatty acyl-coA or triglycerides inside the cells.

It's unclear how FFA could reach STAT3? In Fig. 6, the authors need to show that any effects of FFAs are abolished in STAT3 KO macrophages. In addition, what's o and p (and their concentrations) in Fig. 6G?

Response: Thank you for providing concrete suggestions regarding the mechanism of STAT3 activation. The point-by-point responses are as follows:

(1) What were the FFAs and concentrations used: The concentrations of FFAs have been included in method part of the revised manuscript (Page 30 line 614-616).

(2) Fatty acids exist in the forms of fatty acyl-coA or triglycerides inside the cells. It's unclear how FFA could reach STAT3: We would like to clarify the distinction between "*de novo*-synthesized fatty acids" and "free fatty acids (FFAs)". In this study, FFAs (a mixture of oleate and palmitate) were employed as a reagent to elevate intracellular lipid levels, while "*de novo*-synthesized fatty acids" and "*de novo*-synthesized lipids" refer to intracellular lipids, such as fatty acyl-coA, phospholipids, dialycerides, and triglycerides. Within cell cultures, extracellular FFAs will be uptake by macrophages, and subsequently enter lipid metabolism in the forms of fatty acyl-coA [10]. These intracellular lipids may serve as signaling molecules to induce STAT3 activation [11-13]. To avoid confusion, we have amended the manuscript in this revision (Page 17 line 342-346).

(3) In Fig. 6, the authors need to show that any effects of FFAs are abolished in STAT3 KO macrophages: To address this, we have performed new experiments using STAT3 KO macrophages (Supplementary Fig. 12c). The results revealed that STAT3 KO strongly reduce IL-10-induced expression and secretion of reparative factors, including PDGFβ, TGF-β1, and VEGFβ (Supplementary Fig. 12d, e). Furthermore, the effects of C75 or FFAs are significantly abolished in STAT3 KO macrophages (Supplementary Fig. 12e, f). These results reveal that intracellular lipids induce reparative function by activating STAT3 in macrophages. The corrections have been marked by yellow highlight (Page 17 line 349-352)

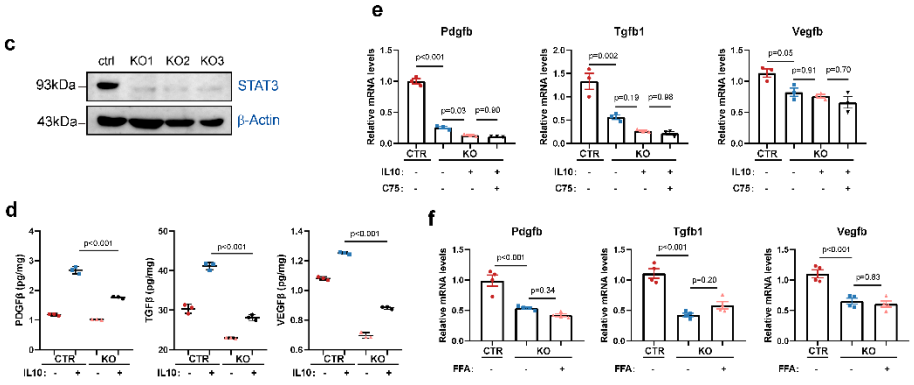

Supplementary Fig. 12 c-e (c) Western blotting analysis of STAT3 expression in STAT3-knockout (KO) RAW264.7 macrophages. (d) The concentration of PDGFβ, TGF-β1 and VEGFβ in STAT3-KO cells in response to IL-10 is determined by ELISA (n = 3). Data were analyzed by a two-tailed Student's t-test. (e) Relative mRNA levels of *Pdgfb*, *Tgfb1* and *Vegfb* in STAT3-KO cells stimulated with C75 in response to IL-10. mRNA amounts normalized relative to *Rplp0* (n = 3). Data were analyzed by a one-way ANOVA followed by a Tukey's multiple comparisons test. (f) Relative mRNA levels of *Pdgfb*, *Tgfb1* and *Vegfb* in STAT3-KO cells

in response to FFAs (100 μM). mRNA amounts normalized relative to *Rplp0* (n = 4). Data were analyzed by a one-way ANOVA followed by a Tukey's multiple comparisons test.

(4) What's o and p (and their concentrations) in Fig. 6G: We have changed the o (oleate) or p (palmitate) to their full name to avoid confusion (Fig. 6g). The concentrations of oleate and palmitate have been included in method part of the revised manuscript (Page 30 line 614-616).

4. In Fig. 7, the CDDO treatment should be repeated to include PPARgKO and PPARa/a models to show the specificity.

Response: To address this question, we have performed additional experiments using PPARγ WT, PPARγ T166A overexpressed and PPARγ KO RAW264.7 cells. PPARγ KO significantly abolished CDDO induced lipid synthesis activity and reparative phenotype (Supplementary Fig. 14a-c), suggesting that CDDO promotes macrophages reparative phenotype through activating PPARγ. In line with our original results, lipid synthesis and reparative phenotype were strongly induced in PPARγ WT overexpressed RAW264.7 cells after CDDO stimulation (Supplementary Fig. 14d-f). However, CDDO treatment did not further increased the reparative phenotype and lipid anabolism in PPARγ T166A cells (Supplementary Fig. 14d-f). Together, these data revealed that CDDO induces macrophages reparative phenotype through PPARγ T166 dephosphorylation. The corrections have been marked by yellow highlight (Page 19 line 393-398). Besides, a similar question regarding CDDO specificity in terms of its Nrf2 activation was made by reviewer #3. Please refer to our response to point 14 from reviewer #3.

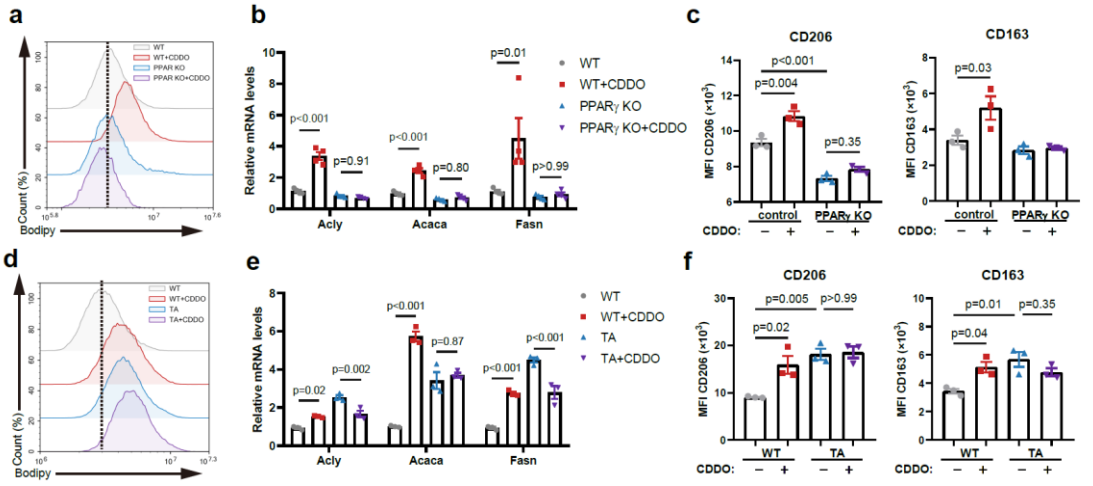

Supplementary Fig. 14 a-f (a) BODIPY 493/503 staining analysis by flow cytometry in PPARγ-WT or PPARγ-KO RAW 264.7 cells in response to CDDO. (b) Relative mRNA levels of lipid synthesis-related genes in PPARγ-WT or PPARγ-KO RAW 264.7 cells in response to CDDO. n = 4 biological replicates per group. Data were analyzed by a one-way ANOVA followed by a Tukey's multiple comparisons test. (c) The expression levels of CD163 and CD206 in PPARγ-WT or PPARγ-KO RAW 264.7 cells in response to CDDO were assessed by flow cytometry. Data are presented as the mean ± s.e.m. of n = 3 biological replicates per group. Data were analyzed by a one-way ANOVA followed by a Tukey's multiple comparisons test. (d) BODIPY 493/503 staining analysis by flow cytometry in PPARγ-WT or PPARγ-TA RAW 264.7 cells in response to CDDO. (e) Relative mRNA levels of lipid

synthesis-related genes in PPARγ-WT or PPARγ-TA RAW 264.7 cells in response to CDDO. *n* = 3 biological replicates per group. Data were analyzed by a one-way ANOVA followed by a Tukey's multiple comparisons test. (f) The expression levels of CD163 and CD206 in PPARγ-WT or PPARγ-TA RAW 264.7 cells in response to CDDO were assessed by flow cytometry. Data are presented as the mean ± s.e.m. of *n* = 3 biological replicates per group. Data were analyzed by a one-way ANOVA followed by a Tukey's multiple comparisons test.

5. The following information should be provided: (1) p7, the source of public transcriptomes of M(IL10); (2) Fasn KO, PPARKO and PPARa/a macrophages and/or mice; (3) how many genes used for SCENIC analysis in Fig. 3A, etc.

Response: Thank you for pointing out the missing information. The following information has been provided in the revised manuscript: **(1)** The source of public transcriptomes of M(IL10) has been included in Supplementary Table 2 in the initial submission, and has been added to the figure legend in the revised manuscript (Page 56 line 1174). **(2)** The method of Fasn KO and Pparg KO has been included in method part of the original manuscript, the gRNA sequences have been provided in Supplementary Table 1 in the initial submission. We have included the information of Stat3 KO and Nrf2 KO in the revised manuscript. We have also provided detailed information to describe this method. Furthermore, the generation of PPARγ$^{A/A}$ mice and the isolation of PPARγ$^{A/A}$ BMDMs have been included in the method part of the original manuscript, which we believe adequately describes these experimental details. **(3)** The gene number used in SCENIC analysis has been included in method part (Page 35 line 723-724).

Reviewer #2:

This is a very nice manuscript looking at the role of PPARg and associated lipid activated STAT3 on macrophage function in several injury models, namely wound repair. It is mechanistic and well written; however, I have the following comments that I think will strengthen the findings and broaden the conclusions.

Response: We thank you for the positive appraisal of our work.

1. For Figure 1, how were monocyte-macrophages defined? Further, what time points post injury were the harvests obtained -- phase 2 is rather broad and many would suggest that days 3-5 is still a transitional period, hence examining early/middle/late may allow for seeing the transition of macrophages.

Response: We used classical marker genes such as *Cd68*, *Lyz2*, *Adgre1*, *Apoe*, *Tgfbr1* to identify monocyte-macrophages. Marker genes provided by the source article of each dataset and SingleR annotation package were also used in cell type annotation. Upon injury, a large number of monocytes infiltrate the wound tissues and undergo a transition to become macrophages. Thus, it is difficult to isolate macrophages from infiltrated monocytes in scRNA-seq analysis. We believe that the term “monocyte-macrophages” would be more appropriate to describe these cell clusters. For the phase

I/II definition, a similar question was made by reviewer #1 and thus this question is addressed in response to question 1(3) from reviewer #1. We have provided some evidence at the end of the letter for you and other reviewers to verify the definition of phases (Reviewer Only Table 3). Besides, we agree with you regarding the theory of wound healing phase transition. However, multiple timepoints are not available for each dataset, and definition of "early/middle/late" timepoints across various tissues would be difficult. As far as we concerned, the definition of pro-inflammatory and reparative phase would be better for data integration in this situation.

2. For Fig 2/3, RNA seq of the actual wound macrophages - isolated at an early/late time point would yield more relevant information than sequencing BMDMs and would be more representative of the plasticity that exists within the wound tissues.

Response: We understand the concerns that BMDMs do not accurately represent the wound healing processes. To address your concerns, we have performed a new RNA-seq analysis using skin wound macrophages and observed increased FAS activity in PPARγ$^{A/A}$ skin wound macrophages compared to PPARγ$^{+/+}$ in reparative phase (Fig. 3e and Supplementary Fig. 7c, d). Consistent with the RNA-seq in BMDMs, this RNA-seq revealed that PPARγ T166A mutation enhanced lipid anabolism in skin wound macrophages. The corrections have been marked by yellow highlight (Page 11 line 226-230, Page 59 line 1230-1231).

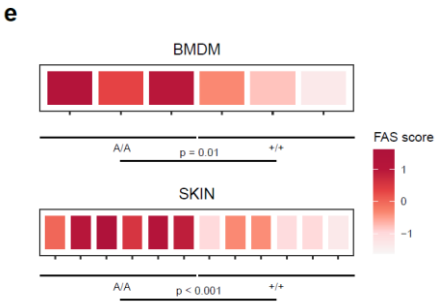

Fig. 3e Heatmap showing expression patterns of FAS-associated signature genes between PPARγ$^{+/+}$ and PPARγ$^{A/A}$ BMDMs or skin wound macrophages (6 dpi). Data were analyzed by a two-tailed Student's t-test.

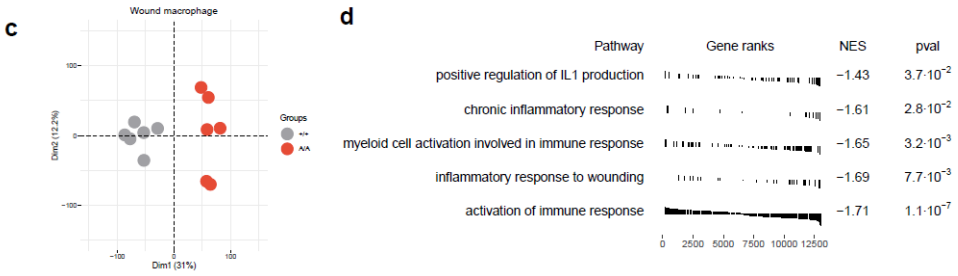

Supplementary Fig. 7c, d (c)PCA of RNA-seq data from PPARγ$^{+/+}$ and PPARγ$^{A/A}$ 6 dpi wound macrophages with 6 biological replicates. (d)GSEA analysis showing the enrichment of indicated GO terms between PPARγ$^{+/+}$ and PPARγ$^{A/A}$ 6 dpi wound macrophages. Genes were ranked by log2FC in the comparison of PPARγ$^{A/A}$ against PPARγ$^{+/+}$ samples.

In Figure 2 of original manuscript, we performed lipidomics to BMDMs to illustrate the upregulation of lipid anabolism in reparative macrophages. To obtain sufficient lipids for lipidomics, a minimum of 5×10^6 cells is required per sample. However, less than 5×10^5 $F4/80^+$ macrophages can be isolated from skin wound per mice. The utilization of a large number of mice for lipidomics analysis may contradict the principles of 3Rs (Reduction, Refinement, and Replacement) in humane animal research. To address this, we opted to use BMDMs instead to perform lipidomics. Additionally, we observed increased lipid accumulation in macrophages from skin wound tissues in reparative phase (Supplementary Fig. 3b). We also conducted western blotting analyses to assess the expression of the rate-limiting enzyme involved in lipid anabolism using wound-derived macrophages (Supplementary Fig. 3d). These results support our findings in BMDMs that FAS activity increased in reparative macrophages.

3. For Fig 4 in the PPAR overexpressers, these assays need to be analyzed in wound macrophages in order to truly represent the changes in the tissue - BMDMs do not accurately depict the tissue changes.

Response: We apologize for the lack of clarity in Figure 4 in the original manuscript. We did not perform experiments using PPARγ overexpressers in this figure. We used $PPAR\gamma^{+/+}$, $PPAR\gamma^{A/A}$ mice and wound isolated cells to examine the role of PPARγ T166 dephosphorylation in the tissue repair function of macrophages (Fig. 4a-c, e, f). Wound tissues from 4 timepoints were used to illustrate the changes of PPARγ T166 phosphorylation levels during wound healing (Fig. 4d). A migration test and phenotype analysis were performed using BMDMs to validate the results of the animal study mentioned above (Fig. 4g, h). Besides, we would like to clarify that we have included both *in vitro* and *in vivo* macrophages to support most of our hypothesis and conclusion in the original manuscript, except for the experiments that require numerous cells as input, such as lipidomics, ^{13}C tracing, and ChIP-seq. We believe that our data adequately support our hypotheses and conclusions.

4. The acute wound healing model used does not accurately represent how human wounds heal - would need splinted/casted model to prevent contraction healing and show these changes in wound repair are relevant to human disease.

Response: It is a great question. Mouse models are valuable to understanding basic mechanisms of wound healing. However, mice are animals with loose skin, which exhibits a histological structure that is different from human skin [14, 15]. Upon injury, mice exhibit accelerated wound closure due to their capacity to contract the wound in the early stage of wound healing [15]. This limitation is challenging for researchers using mouse models to study wound healing process. We have tried various strategies to overcome it, and we are delighted to share our experience with you here.

Silicone rings are widely used for reducing contraction of mouse wounds. We customized a batch of silicone rings, and secured the rings to the dorsal skin of mice by 8 sutures around the perimeter. Then, an excisional wound was made in the center of the circle (Reviewer Only Fig. 1a). However, during wound healing process, we observed a fairly high rate of ring loss, primarily due

to the self-grooming of mice. Indeed, it is the main drawback of this type of ring method. To solve this problem, we attempted to refix the ring around the wound site, but the surgery resulted in severe secondary injury, which significantly impacts the experimental results. Inspired by the recovery cones for dogs and cats after surgery, we decided to use mouse cones to prevent ring loss (Reviewer Only Fig. 1b). During the wound healing process, the mice exhibit signs of irritability, accompanied by a decrease in water and food consumption as well as reduced activity levels. We have made the decision to discontinue this plan. The final approach we adopted in this study is a tape model. In brief, we utilized an inelastic medical adhesive tape to securely affix the dorsal skin of mice, and subsequently created excisional wounds (Reviewer Only Fig. 1c). Experientially, the tape can prevent the wound contraction within 3-5 days, during which the contraction process is intensified. Considering that the anchoring sutures will serve as the main points of skin fixation in the ring model, our method ensures skin fixation in all directions, effectively preventing wound contraction. The limitation mainly lies in its incomplete resolution of wound contraction. We have used the tape method in the original manuscript, except for Figure 4A-C of the original manuscript. We have performed additional experiments using tape method to replace these figures (Fig. 4b, c). The corrections have been marked by yellow highlight (Page 26 line 536-539, Page 60 line 1254).

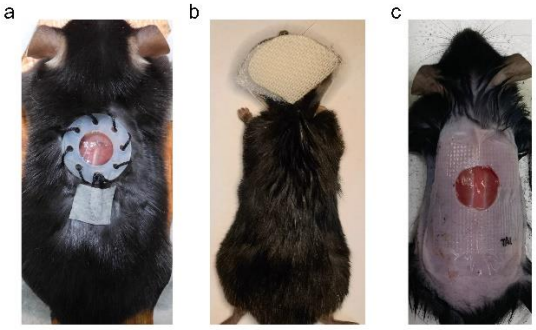

Reviewer Only Fig. 1 Skin injury models. (a) Silicone ring model. (b) The usage of mouse cone. (c) Medical tape model.

We agree with your concerns regarding the acute skin injury model without splinting strategies, although this model is widely used in the mechanism study of wound healing [16-18]. To further strengthen the animal studies, we have included two additional classical wound healing models including skeletal muscle injury and liver injury models in this revision. We triggered skeletal muscle damage of mice by intramuscular injection of the snake venom, Cardiotoxin (CTX). We observed a high number of immune cell infiltration at 2 days post injection, which were controlled around 8 dpi (Supplementary Fig. 4a). The cross-sectional area (CSA) of the regenerating muscle fibers was significantly larger at 8 dpi (Supplementary Fig. 4b). We induced a reversible acute liver injury through a single dose of CCl_4 injection. CCl_4 led to severe liver damage and significant upregulation of serum alanine aminotransferase (ALT) and aspartate aminotransferase (AST) activities at 1 dpi, which were controlled around 4 dpi (Supplementary Fig. 4c, d). Next, we isolated the macrophages from the wound tissues of these models. Consistent with our finding in skin injury, macrophages from both liver and muscle injury exhibited enhanced lipid synthesis activities during

the reparative phase (Supplementary Fig. 4e-h), indicating a strong correlation between lipid synthesis and reparative function of macrophages. The information has been added to revised manuscript and marked by yellow highlight (Page 8 line 158, 164, Page 9 line 173-180).

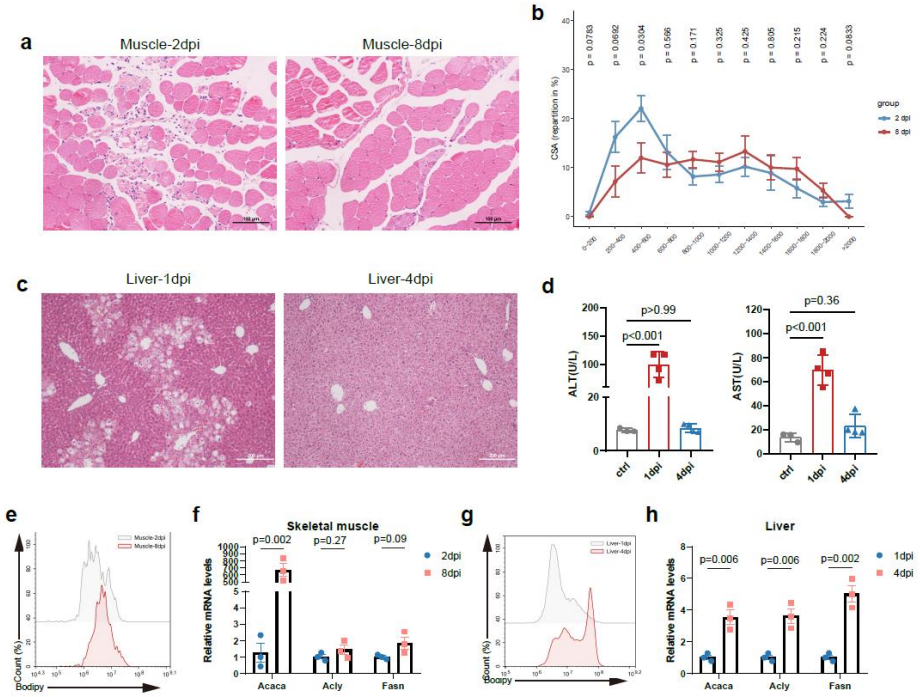

Supplementary Fig. 4 (a) Representative H&E images of 2 dpi and 8 dpi muscle sections. Scale bar, 100 μm. (b) Repartition of fiber cross section area (CSA) at 2 dpi and 8 dpi. Data indicated mean ± s.e.m. of $n = 6$ biological replicates. Data were analyzed by a two-tailed Student's t-test. (c) Representative H&E images of 1 dpi and 4 dpi liver sections. Scale bar, 200 μm. (d) Serum ALT and AST levels in control ($n = 3$), 2 dpi and 8 dpi mice. Data is presented as mean ± s.e.m. of $n = 4$ biological replicates. Data were analyzed by a one-way ANOVA followed by a Dunnett's multiple-comparisons test. (e) BODIPY 493/503 staining analysis by flow cytometry in MACS-sorted muscle macrophages ($F4/80^+$) from 2 dpi and 8 dpi mice. (f) Relative mRNA levels of lipid synthesis-related genes in MACS-sorted muscle macrophages ($F4/80^+$) from 2 dpi and 8 dpi mice. $n = 3$ biologically independent mice per group. Data were analyzed by a two-tailed Student's t-test. (g) BODIPY 493/503 staining analysis by flow cytometry in MACS-sorted liver macrophages ($F4/80^+$) from 1 dpi and 4 dpi mice. (h) Relative mRNA levels of lipid synthesis-related genes in MACS-sorted liver macrophages ($F4/80^+$) from 1 dpi and 4 dpi mice. $n = 3$ biologically independent mice per group. Data were analyzed by a two-tailed Student's t-test.

Moreover, using these injury models, we found that the CSA of muscle fibers was significantly larger in the $PPAR\gamma^{A/A}$ mice compared to $PPAR\gamma^{+/+}$ mice on 8 days post CTX injection (Supplementary Fig. 9a, b). In acute liver injury models, CCl_4-induced serum ALT and AST activities were significantly higher in $PPAR\gamma^{+/+}$ mice on 4 dpi (Supplementary Fig. 9c, d). Besides, wound tissues from $PPAR\gamma^{A/A}$ mice showed a higher abundance of reparative macrophages in both muscle and liver injury models (Supplementary Fig. 9e, f). These results further validated that $PPAR\gamma^{A/A}$ mutation significantly accelerated wound healing process after injuries. The information has been added to revised manuscript and marked by yellow highlight (Page 13 line 253-260).

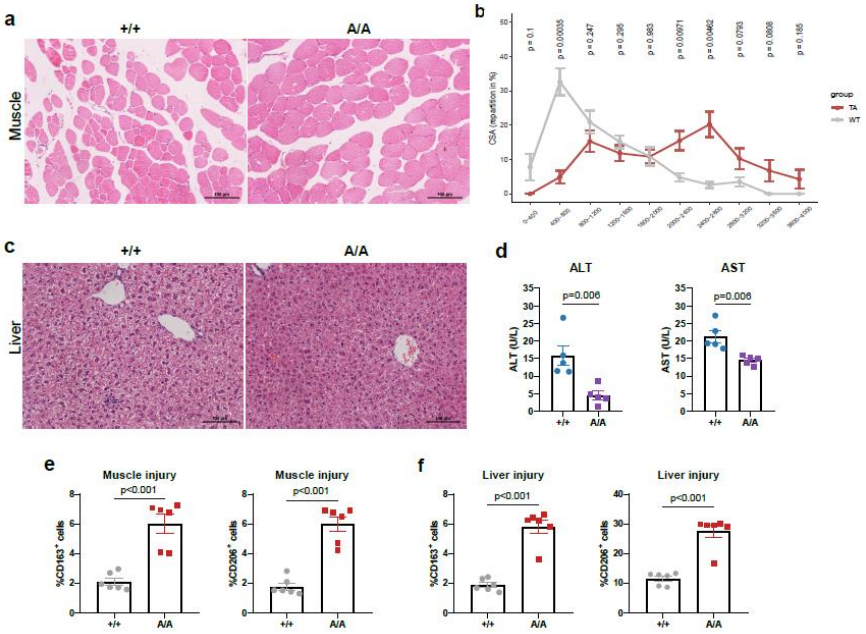

Supplementary Fig. 9 (a) Representative H&E images of 8 dpi muscle sections from PPARγ$^{+/+}$ and PPARγ$^{A/A}$ mice. Scale bar, 100 μm. (b) Repartition of fiber CSA in PPARγ$^{+/+}$ and PPARγ$^{A/A}$ mice at 8 dpi. Data indicated mean ± s.e.m. of $n = 6$ biological replicates. Data were analyzed by a two-tailed Student's t-test. (c) Representative H&E images of 4 dpi liver sections from PPARγ$^{+/+}$ and PPARγ$^{A/A}$ mice. Scale bar, 100 μm. (d) Serum ALT and AST levels in PPARγ$^{+/+}$ and PPARγ$^{A/A}$ mice at 4 dpi. Data is presented as mean ± s.e.m. of $n = 5$ biological replicates. Data were analyzed by a two-tailed Student's t-test. (e) Expression of the CD163 and CD206 in 8 dpi muscle from PPARγ$^{+/+}$ and PPARγ$^{A/A}$ mice were assessed by flow cytometry. The quantification of percentage of CD163+ and CD206+ macrophages from $n = 6$ biological replicates is presented as the mean ± s.e.m. Data were analyzed by a two-tailed Student's t-test. (f) Expression of the CD163 and CD206 in 4 dpi liver from PPARγ$^{+/+}$ and PPARγ$^{A/A}$ mice were assessed by flow cytometry. The quantification of percentage of CD163+ and CD206+ macrophages from $n = 6$ biological replicates is presented as the mean ± s.e.m. Data were analyzed by a two-tailed Student's t-test.

Furthermore, considering that this study mainly focuses on reparative mechanism of macrophages, we have conducted additional experiments using human macrophages in the revised manuscript to demonstrate the therapeutic effect of CDDO to human wounds. The results shows that CDDO treated macrophages significantly promoted human skin fibroblasts (HSF cell line) and human epidermal keratinocytes (HaCaT cell line) migration (Supplementary Fig. 15b, c). Collectively, we believe that these findings are sufficient to prove the therapeutic effects of CDDO in mouse and human wound healing. The corrections have been marked by yellow highlight (Page 20 line 412-416).

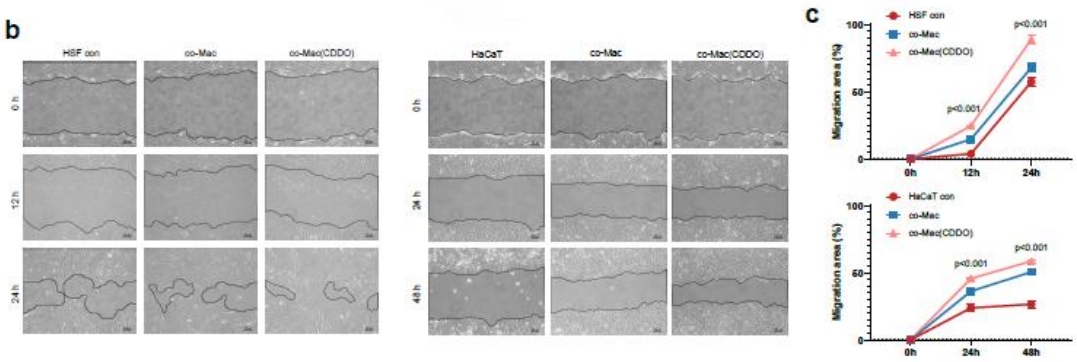

Supplementary Fig. 15b, c (b) The scratch wound representative images of HSF and HaCaT cells co-cultured with human macrophages (Mac) or CDDO pretreated Mac with for 48 hours. Scale bar, 100 μm. (c) The scratch wound closure rate of HSF and HaCaT cells co-cultured with human Mac or CDDO pretreated Mac (n = 3 per group). Data were analyzed by a one-way ANOVA followed by a Dunnett's multiple-comparisons test.

Reviewer #3:

General impression

Macrophages remain an important immune cell player during the wound healing process. Yet, much less is known about the molecular mechanisms governing macrophage metabolic and phenotypic plasticity in driving wound reparation. The manuscript describes a molecular mechanism involving PPARγ-mediated metabolic reprogramming that facilitates the maturation of reparative macrophages during wound healing. Through a series of in vitro and in vivo experiments, it was revealed that T166 dephosphorylation of PPARγ during the recovery stage promotes lipogenesis in macrophages for the expansion of endoplasmic reticulum, subsequently increasing the secretion of STAT3-induced growth factors like Tgfb1, Vegfb and Pdgfb to promote wound closure. Furthermore, Zuo et al. demonstrated the clinical translatability of this work using topical application of CDDO which inhibits PPARγ T166 phosphorylation. The following points highlight my concerns:

Response: We would like to thank you for the positive evaluation and thorough review of our work. Your comments have been very helpful and have encouraged us to perform additional experiments to strengthen our findings. Below we detail how we have addressed your concerns point-by-point.

Major comments

1. The title should be revised to "PPARγ T166 dephosphorylation…" to reflect the exact regulatory mechanism.

Response: Thanks for your suggestion, the title has been revised and the corrections have been marked by yellow highlight (Page 1 line 1).

2. In Figure 1 and S1A-C, it is unclear how the macrophages from scRNAseq of different tissues were classified into phase I (acute injury stage) and phase II (reparative stage). Acute injuries in different types of tissues are likely to have different rates of recovery. For instance, dermal injuries tend to heal faster compared to spinal cord or muscle injuries. Therefore, the criteria to distinguish

the acute and reparative phases in all tissue injuries should be outlined. Further, some models were of different types of sequencing experiments (e.g. single cell nature, bulk, or macrophage isolated only). How did the authors reconcile the differences?

Response: For the phase I/II definition, a similar question was made by reviewer #1 and thus this question is addressed in response to question 1(3) from reviewer #1. We have provided some evidence at the end of the letter for you and other reviewers to verify the definition of phases (Reviewer Only Table 3). Further, the selection of sequencing method mainly based on the experimental purpose. For instance, in order to evaluate the metabolism of macrophages during wound healing, we performed scRNA-seq atlas that allows us to comprehensively analyze the metabolic changes in different wound tissues. scRNA-seq detects gene expression levels in each cell, making it suitable for studying the heterogeneity and phenotype transition of macrophages during wound healing. To analyze reparative macrophages *in vitro*, bulk RNA-seq of polarized macrophages would be the optimal choice. Because cultured macrophages exhibit lower heterogeneity. Additionally, considering the substantial dropout rate observed in scRNA-seq, bulk RNA-seq emerges as a more suitable approach for investigating gene expression levels. This combination of multi-omics enables us comprehensively analyze macrophages metabolism *in vitro* and *in vivo*.

3. In Figure 1C, it is unclear what the "Gene number" 34, and 8 numbers mean. The authors should indicate with much greater clarity on the meaning and derivations of the terms gene number, and the quantities of 34 and 8.

Response: Thanks for your suggestions in terms of figure legends. In Fig. 1c, we performed a Gene Ontology (GO) enrichment analysis to the differential expressed genes in the comparison between the phase I and phase II skin wound macrophages. This figure shows the correlation between highly enriched GO terms and related genes. Pie charts represent enriched biological processes and the ratio of gene number that enriched in each group, small dots represent genes associated with the processes. The size of each pie indicates the number of genes enriched in a specific term. "Gene number" 34, and 8 are the legend of pie size that was automatically generated by the tools. The corrections have been marked by yellow highlight (Page 56 line 1160-1163).

4. The authors should indicate what the values stated in Figure 1E, meant. In the legend, it is stated high, low but not what values these represent. This comment applies to other figures of similar nature.

Response: A similar question was made by reviewer #1 and thus this question is addressed in response to question 1(4) from reviewer #1.

5. It is unclear which model Figure 1F is referring to. Is it a pseudotime analysis? Although the main text (line 127) alludes to Figure 1F representing the skin macrophages, but the UMAP visualized in Figure 1F is vastly different from that of Figure 1B.

Response: Fig. 1b presents a uniform manifold approximation and projection (UMAP) plot of SKIN dataset, demonstrating distinct expression patterns between macrophages in phase I and phase II. Fig. 1f is a pseudotime analysis of macrophages of SKIN dataset, which showed the phenotype transition of macrophages during wound healing process. We employed monocle R package for conducting this pseudotime analysis. Monocle is extensively employed in the analysis of cell trajectory in scRNA-seq [19]. This tool ordered single cells in pseudotime, and placed them along a trajectory. Thus, the visualization is different between Fig. 1b and Fig. 1f.

6. In Figure 1F, the method to annotate different subtypes of macrophages in phase I and II, i.e. M0, M(IFNg), M(LPS), M(IL4) and M(IL10), is not elaborated. Any particular reason why M(IFNg) is missing in Figure 1G? Ideally, the colors for different macrophage subpopulations in Figure 1F and G should be consistent to avoid confusion.

Response: We have included the annotation method in the revised manuscript (Page 34-35 line 709-719). We would like to apologize for this oversight. As Fig. 1f shows, macrophages from inflammatory phase exhibited a phenotype resembling M(LPS) rather than M(IFNγ). Thus, M(IFNγ) was excluded from further analysis (Fig. 1g). Besides, as you suggested, we have amended the colors for different macrophage subpopulations in Fig. 1f and Fig. 1g to avoid confusion.

7. While Figure 1C & E are derived from scRNAseq of different tissues, validation of the role of reparative macrophages was primarily conducted using skin injury in mice models and scratch tests using dermal fibroblasts. Hence, it is cautious not to over-generalize the findings beyond the dermal injury context, especially in the discussion and conclusion.

Response: We agree with your concerns. To strengthen our animal studies, we have included 3 injury models, including skin, muscle and liver injuries, in the revised manuscript to validate the results of the scRNA-seq atlas. We have conducted new experiments using these models to demonstrate the reparative effects of PPAR$\gamma^{A/A}$ mutation. The original manuscript already discussed the results of skin injury model, while additional information regarding muscle and liver injuries has been provided in response to question 4 from reviewer #2. We have also revised the discussion and conclusion to avoid over-generalization when only skin injury was used. The corrections have been marked by yellow highlight (Page 8 line 158, 164, Page 24 line 503).

8. The visualization of Figure 1G and 3E is confusing. It is unclear what the values represent. The error bars are also erroneous. What statistical test is used for the comparisons?

Response: We apologize for the inconvenience caused by this visualization. We have changed these figures to heatmap to avoid confusion (Fig. 1g, Fig. 3e). The corrections have been marked by yellow highlight (Page 56 line 1172-1174, Page 59 line 1230-1231). We believe that these changes will help you and readers easily understand the meaning conveyed by these plots.

9. Figure S6A reveals possible accumulation of lipid droplets (white circular structures) in the dermis layers.

Response: We have checked the experimental records and found that the accumulation of adipocytes mainly results from the usage of mice in different hair cycle of skin. Periodical remodeling is one of the most distinguishing features of dermal white adipose tissue (dWAT). This process involves significant thickening of dWAT around anagen hair follicles and subsequent thinning during the transition from catagen to telogen stages [20, 21]. To avoid confusion, we have conducted new experiments using the mice from the same hair cycle stage, and changed the H&E plots in Supplementary Fig. 8a. The H&E images showed no significant difference in terms of lipid accumulation in skin tissues between PPARγ$^{+/+}$ and PPARγ$^{A/A}$ mice.

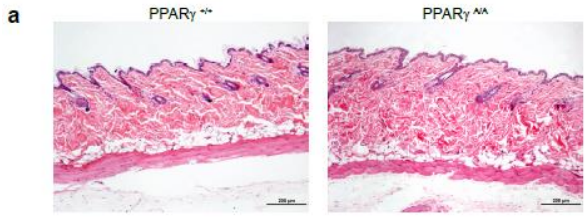

Supplementary Fig. 8 (a) H&E staining of skin from 2-month-old PPARγ$^{+/+}$ and PPARγ$^{A/A}$ mice.

10. Did the SCENIC analysis also predict increased activity of STAT3 in reparative wound macrophages?

Response: It is an interesting question. We have performed this analysis and found that the STAT3 activity significantly upregulated in macrophages at reparative phase (Reviewer Only Fig. 2). This result is consistent with our initial findings, which demonstrated that *de novo*-synthesized lipids enhance reparative function of macrophages by activating STAT3.

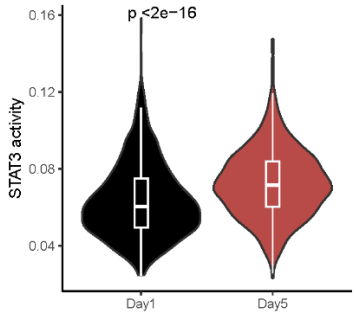

Reviewer Only Fig. 2 Violin plot of STAT3 activity at phase I/II in skin wound healing.

11. In Figure 6F-G, it is better to show fold change instead of change in CT values to avoid confusion.

Response: Thanks for your suggestion. The CT values have been converted to fold enrichment to avoid confusion (Fig. 6f, g).

12. In Page 16, Lines 328-329, it is important to demonstrate that the increased lipogenic products from phospholipid synthesis are directed to endoplasmic reticulum expansion. Tracing with [U-13C]

glucose followed by endoplasmic reticulum isolation could potentially provide valuable insight. Furthermore, the data suggests a correlation between ER expansion and secretion of reparative proteins in reparative macrophages. To ascertain a causal relationship, the levels of reparative signals when ER expansion is inhibited should be examined.

Response: We thank you for your concrete suggestions with regard to metabolic tracing. We have conducted new experiments that use [U-^{13}C]-labeled glucose to trace the fate of *de novo*-synthesized lipids. As Supplementary Fig. 13g shows, IL-10 treatment and T166A mutation strongly upregulated the isotope ratio of $^{13}C/^{12}C$ in ER, indicating that the lipogenic products are directed to ER expansion. The corrections have been marked by yellow highlight (Page 19 line 379-381, Page 41 line 848-853).

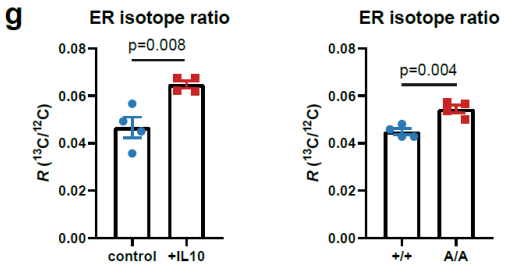

Supplementary Fig. 13 (g) The $^{13}C/^{12}C$ isotope ratio of ER from M(IL10) or PPARγ$^{+/+}$ and PPARγ$^{A/A}$ BMDMs. $n = 4$ biological replicates per group. Data were analyzed by a two-tailed Student's t-test.

Furthermore, we understand your concerns with regard to the correlation between ER expansion and secretion of reparative proteins. Reparative proteins, such as Vegfb and Pdgfb, are classical secretory proteins that are secreted into the extracellular space via conventional protein secretion (CPS) pathway, in which ER plays a crucial role in protein translation, processing and transportation. The correlation between ER expansion and protein secretion capacity has been fully studied previously [22-24]. As far as we know, the term "ER expansion" has been used directly to indicate the protein secretion capacity of cells [25]. To address your concerns, we used Brefeldin A (BA) to block the transport of secreted proteins from ER to Golgi apparatus. ELISA showed that BA significantly abolished IL-10-induced PDGFβ and TGF-β1 secretion in macrophages (Reviewer Only Fig. 3a, b), indicating the causal relationship between ER function and reparative protein secretion.

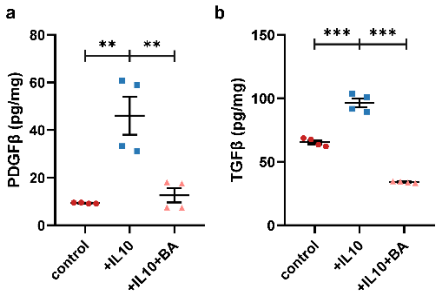

Reviewer Only Fig. 3 The correlation between ER expansion and protein secretion. (a, b) Secretion of TGF-β1 and PDGFβ in cell culture medium is determined by ELISA upon indicated stimulation.

13. The GEO accession numbers of RNAseq, CHIP-seq and CUT&RUN-seq should be provided.

Response: The GEO accession has been added to the revised manuscript. The corrections have been marked by yellow highlight (Page 47 line 969-976).

14. Apart from being a PPARγ T166 phosphorylation inhibitor, bardoxolone (CDDO) is also a strong inducer of Nrf2 (PMID 34052830). Therefore, additional control groups/evaluations are needed to validate that the benefits are not confounded by Nrf2 signaling.

Response: To validate CDDO treatment are not confounded by Nrf2 signaling, we knocked out *Nrf2* by CRISPR-cas9 or reduced *Nrf2* expression by shRNA in Raw264.7 cells (Supplementary Fig. 14g). The results showed that the expression levels of *Nrf2* did not influence CDDO-induced lipid synthesis and reparative phenotype (Supplementary Fig. 14h, i). The information has been added to revised manuscript and marked by yellow highlight (Page 19-20 line 398-401). Besides, a similar question regarding CDDO specificity in terms of its PPARγ activation was made by reviewer #1. Please refer to our response to question 4 from reviewer #1.

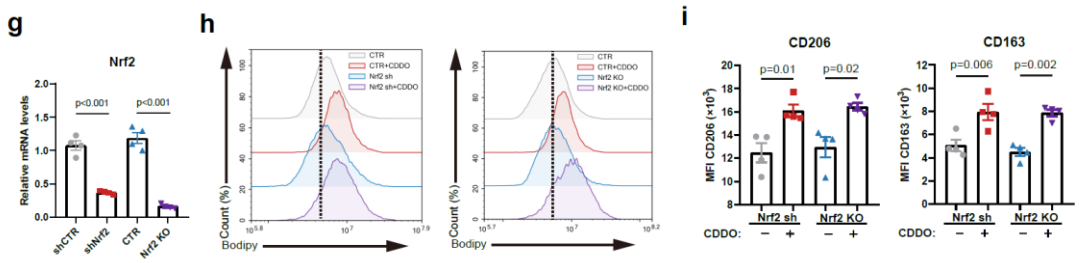

Supplementary Fig. 14g-i (g) Relative mRNA levels of *Nrf2* (*Nfe2l2*) in shCTR, shNrf2 and Nrf2 KO RAW 264.7 cells. $n = 4$ biological replicates per group. Data were analyzed by a two-tailed Student's t-test. (h) BODIPY 493/503 staining analysis by flow cytometry in shNrf2 or Nrf2 KO RAW 264.7 cells in response to CDDO. (i) The expression levels of CD163 and CD206 in shNrf2 or Nrf2 KO RAW 264.7 cells in response to CDDO were assessed by flow cytometry. Data are presented as the mean ± s.e.m. of $n = 4$ biological replicates per group. Data were analyzed by a one-way ANOVA followed by a Tukey's multiple comparisons test.

Minor comments

15. Error in Line 139 – Figure 2G should be Figure 1G.

Response: Thank you for pointing out. The corrections have been marked by yellow highlight (Page 7 line 137, 140).

16. For Figure 1G, authors should indicate what datasets were used and how the analyses were done.

Response: The datasets used in Fig. 1g have been included in legends of revised manuscript. We have changed Fig. 1g to heatmap to avoid confusion. The R scripts used to generate this figure have

been submitted to GitHub. The corrections have been marked by yellow highlight (Page 56 line 1174).

17. Figure 3H, typo on x-axis, Bodioy should be Bodipy.

Response: The x-axis label has been corrected (Fig. 3h).

18. For Figure S5B, it is unclear how the genes were ranked. Are the gene ranked by comparing PPARg+/+ against PPARgA/A or the inverse?

Response: The genes were ranked by comparing their expression levels of PPARγ$^{A/A}$ against PPARγ$^{+/+}$ samples. A positive normalized enrichment score (NES) indicates a high enrichment of the term in PPARγ$^{A/A}$, a negative NES suggests a high enrichment of the term in PPARγ$^{+/+}$ group. We have amended the figure legends in the revised manuscript (Supplementary Fig. 7b, d).

19. In Page 9 Line 176, it should be "… the pro-migratory ability of dermal fibroblasts M(IL10) …".

Response: We understand the concerns of you regrading to this sentence. The sentence has been modified to *"Importantly, both FASN inhibition and Fasn knockout in M(IL10) decreased dermal fibroblasts migration in scratch tests"* (Page 9 line 187-188).

20. In Fig. S4E, quantification of the fluorescence intensities and statistical analysis should be shown.

Response: The mean fluorescence intensity (MFI) has been added to this figure (Supplementary Fig. 6e).

21. In Page 10 Line 205, it should be "…through dephosphorylating T166 site…".

Response: Thanks for bringing that to our attention. The corrections have been marked by yellow highlight (Page 11 line 219). Besides, manuscript has been revised to prevent any similar omissions (Page 21 line 430, Page 58 line 1214).

Reviewer #4 (Remarks to the Author):

My review concentrates on the reproducibility of the bioinformatics analysis outlined in this manuscript, with a particular attention at the high-throughput technologies discussed.

Major:

1) The paper mentions that RNA-seq, ChIP-seq, and CUT&RUN-seq data are currently being uploaded to the Gene Expression Omnibus (GEO) database, emphasizing data availability. Authors are required to specify the superseries of the data in the manuscript and provide access tokens to reviewers.

Response: The GEO accession and the tokens for reviewer have been added to the revised manuscript. The corrections have been marked by yellow highlight (Page 47 line 969-976).

2) Single cell data analysis. In the manuscript it is presented the reanalysis of 9 single cell datasets. The description provided in Material and Methods is not sufficient. It is required to authors to provide a github describing the full analysis performed on the datasets.

Response: We have added detailed information to scRNA-seq analysis in the revised manuscript. The R scripts used for scRNA-seq analysis have been submitted to GitHub. A table containing the information of the GEO accession, source article of these datasets, marker genes used to identify macrophage clusters, timepoint of phase I/II, brief study description has been submitted along with the revised manuscript as Supplementary Table 2. The corrections have been marked by yellow highlight (Page 33 line 684-694, Page 34-35 line 709-719, Page 35 line 723-724, Page 47 line 969-976).

3) Github must also include the analysis performed with SCENIC software.

Response: The R scripts used for SCENIC analysis have been submitted to GitHub. The corrections have been marked by yellow highlight (Page 47 line 969-976).

4) In the section RNA sequencing and data analysis, the thresholds, i.e. adj-pvalue and absolute log2FoldChange, used to identify the differentially expressed genes are not indicated.

Response: Sorry for the omission. The thresholds have been included in the method of revised manuscript. The corrections have been marked by yellow highlight (Page 36 line 743-744).

5) The MACS2 analysis results must be also provided in Zenodo or figshare repository.

Response: Thank you for pointing out. The MACS2 analysis results have been submitted to GEO as the supplementary files of ChIP-seq.

6) Bed files generated by the analysis of CUT&RUN-seq must also be provided in Zenodo or figshare repository.

Response: The bed files generated by the analysis of CUT&RUN-seq have been submitted to GEO as supplementary files of CUT&RUN.

7) The code used to generate Fig.1 B, E, F, G, Fig. 3 A, B, E and Fig. 5 A panels must be provided in the github.

Response: The R scripts used to generate these plots have been submitted to GitHub. The corrections have been marked by yellow highlight (Page 47 line 969-976).

Editorial Note: Parts of the table below have been redacted as indicated to remove third-party material where no permission to publish could be obtained.

Reviewer Only Table 3 Evidence for Phase I/II definition.

Model	PMID	Phase I	Phase II	Phase I evidence (Source article)	Phase II evidence (Source article)
LUNG	32678092	10 d	28 d	[REDACTED]	
AWI	33378665	1 d	7 d		
MCIN	35184420	3 d	14 d		
KDI	35821371	3 d	14 d		
SKIN	35210411	1 d	5 d		
ACLI	35967299	1 d	7 d		
SCI	37148871	3 d	7 d		
SMI	35733848	4 d	7 d		
LIVER	35659879	2 d	4-7 d		

The amendments that were not mentioned in response to the reviewers' comments are as follows:

(1) All the plots now display the exact p value instead of using "*/ns" to indicate significance. The amended figures include Fig. 4f, Supplementary Fig. 3c, Supplementary Fig. 5c, Supplementary Fig. 6h, Supplementary Fig. 10a, c, Supplementary Fig. 11d.

(2) The gene name of "Acc1" in Supplementary Fig. 5c has been changed to its symbol name to

avoid confusion.

(3) The colors of sample points of Acaca and Fasn in Fig. 5c have been changed to be consistent with other genes.

(4) The style of figure labels has been changed according to the formatting instructions.

(5) The binding peak plots (Fig. 6a and Supplementary Fig. 12a) were regenerated in vector graphics format using the Gviz R package, replacing the utilization of IGV screenshot.

(6) The script of scRNA-seq has been found to contain a bug that affects the cell count in AWI, KDI, LIVER, MCIN, and SCI datasets. However, it does not impact the overall conclusions (Fig. 1e, Supplementary Fig. 1a-c). The corrections have been marked by yellow highlight (Page 5 line 103).

(7) Supplementary figure legends have been amended according to the changes of plots.

(8) A reagent cat. correction (Page 31 line 638-639).

Reference

1. Wynn, T.A. and K.M. Vannella, *Macrophages in Tissue Repair, Regeneration, and Fibrosis.* Immunity, 2016. **44**(3): p. 450-462.
2. Cheng, S., et al., *A pan-cancer single-cell transcriptional atlas of tumor infiltrating myeloid cells.* Cell, 2021. **184**(3): p. 792-809.e23.
3. Perez, R.K., et al., *Single-cell RNA-seq reveals cell type–specific molecular and genetic associations to lupus.* Science, 2022. **376**(6589).
4. Farah, E.N., et al., *Spatially organized cellular communities form the developing human heart.* Nature, 2024. **627**(8005): p. 854-864.
5. Wu, Y., et al., *Spatiotemporal Immune Landscape of Colorectal Cancer Liver Metastasis at Single-Cell Level.* Cancer Discovery, 2022. **12**(1): p. 134-153.
6. Mantovani, A., et al., *The chemokine system in diverse forms of macrophage activation and polarization.* Trends in Immunology, 2004. **25**(12): p. 677-686.
7. Tang, L., et al., *M2A and M2C Macrophage Subsets Ameliorate Inflammation and Fibroproliferation in Acute Lung Injury Through Interleukin 10 Pathway.* Shock, 2017. **48**(1): p. 119-129.
8. Lu, J., et al., *Discrete functions of M 2a and M 2c macrophage subsets determine their relative efficacy in treating chronic kidney disease.* Kidney International, 2013. **84**(4): p. 745-755.
9. Vannella, K.M. and T.A. Wynn, *Mechanisms of Organ Injury and Repair by Macrophages.* Annual Review of Physiology, 2017. **79**(1): p. 593-617.
10. Deng, L., S. Kersten, and R. Stienstra, *Triacylglycerol uptake and handling by macrophages: From fatty acids to lipoproteins.* Progress in Lipid Research, 2023. **92**.
11. Di Conza, G., et al., *Tumor-induced reshuffling of lipid composition on the endoplasmic reticulum membrane sustains macrophage survival and pro-tumorigenic activity.* Nature Immunology, 2021. **22**(11): p. 1403-1415.
12. Zhang, M., et al., *A STAT3 palmitoylation cycle promotes TH17 differentiation and colitis.* Nature, 2020. **586**(7829): p. 434-439.
13. Mi, Y., et al., *Loss of fatty acid degradation by astrocytic mitochondria triggers neuroinflammation and neurodegeneration.* Nature Metabolism, 2023. **5**(3): p. 445-465.

14. Davidson, J.M., F. Yu, and S.R. Opalenik, *Splinting Strategies to Overcome Confounding Wound Contraction in Experimental Animal Models.* Advances in Wound Care, 2013. **2**(4): p. 142-148.
15. Yampolsky, M., I. Bachelet, and Y. Fuchs, *Reproducible strategy for excisional skin-wound-healing studies in mice.* Nature Protocols, 2023. **19**(1): p. 184-206.
16. Kim, J., et al., *Low-dielectric-constant polyimide aerogel composite films with low water uptake.* Polymer Journal, 2016. **48**(7): p. 829-834.
17. Wang, G., et al., *Bacteria induce skin regeneration via IL-1β signaling.* Cell Host & Microbe, 2021. **29**(5): p. 777-791.e6.
18. Kusnadi, A., et al., *The Cytokine TNF Promotes Transcription Factor SREBP Activity and Binding to Inflammatory Genes to Activate Macrophages and Limit Tissue Repair.* Immunity, 2019. **51**(2): p. 241-257.e9.
19. Trapnell, C., et al., *The dynamics and regulators of cell fate decisions are revealed by pseudotemporal ordering of single cells.* Nature Biotechnology, 2014. **32**(4): p. 381-386.
20. Schmidt, B. and V. Horsley, *Unravelling hair follicle–adipocyte communication.* Experimental Dermatology, 2012. **21**(11): p. 827-830.
21. Guerrero-Juarez, C.F. and M.V. Plikus, *Emerging nonmetabolic functions of skin fat.* Nature Reviews Endocrinology, 2018. **14**(3): p. 163-173.
22. Borgese, N., M. Francolini, and E. Snapp, *Endoplasmic reticulum architecture: structures in flux.* Current Opinion in Cell Biology, 2006. **18**(4): p. 358-364.
23. Federovitch, C.M., D. Ron, and R.Y. Hampton, *The dynamic ER: experimental approaches and current questions.* Current Opinion in Cell Biology, 2005. **17**(4): p. 409-414.
24. van Anken, E., et al., *Sequential Waves of Functionally Related Proteins Are Expressed When B Cells Prepare for Antibody Secretion.* Immunity, 2003. **18**(2): p. 243-253.
25. Everts, B., et al., *TLR-driven early glycolytic reprogramming via the kinases TBK1-IKKε supports the anabolic demands of dendritic cell activation.* Nature Immunology, 2014. **15**(4): p. 323-332.

REVIEWERS' COMMENTS

Reviewer #1 (Remarks to the Author):

The authors have performed new experiments to address most of the concerns from the reviewers. I don't have additional comments.

Reviewer #2 (Remarks to the Author):

The authors have addressed all of my concerns.

Reviewer #3 (Remarks to the Author):

Thank you for your effort in addressing my queries.
I do not have any more comments.

Reviewer #3 (Remarks on code availability):

I have examined the R script for SCENICR and RNAseq.

Reviewer #4 (Remarks to the Author):

The authors addressed all the points I raised.
However, still some work as to be done concerning the reproducibility of the bioinformatics analysis. Please see below the review of the github

Reviewer #4 (Remarks on code availability):

Although the authors did a good work in the github repository. They must add in the readme a detailed indication where to retrieve the data used by each of the script.
The script https://github.com/XiaoXxin/Macrophage_Reparative/blob/main/CUTRUN BMDM STAT3/script_for_CUTRUN.R requires ./BMDM_STAT3.bigWig but the location where to retrieve such file is not indicated anywhere
Same problem apply to https://github.com/XiaoXxin/Macrophage_Reparative/blob/main/ChIPseq BMDM PPARg/script_for_ChIPseq.R which requires ./TA_summits.bed and ./WT_summits.bed but from the github is not possible to identify where those files can be retrieved.
https://github.com/XiaoXxin/Macrophage_Reparative/blob/main/Lipidomics/script_for_lipidomics.R lacks the location of M2c_M0.all.txt
In https://github.com/XiaoXxin/Macrophage_Reparative/blob/main/scRNAseq SCENIC/sc_script_for_SCENIC.R
the path to download from https://resources.aertslab.org "mm9-500bp-upstream-7species.mc9nr.feather", "mm9-tss-centered-10kb-7species.mc9nr.feather" is not complete, it hust points to the main folder.

All scripts should be carefully revised to include the location of the input files. Additionally, the version of R and the R libraries used in each script must be provided.

Dear Editor,

Thank you for your invaluable assistance with our original manuscript (Submission ID: NCOMMS-24-00526A) entitled “Lipid synthesis, triggered by PPARγ T166 dephosphorylation, sustains reparative function of macrophages during tissue repair”. We sincerely appreciate your interest in our work, diligent efforts in handling our paper, and valuable suggestions. The point-by-point responses are as follows:

Reviewer #1 (Remarks to the Author):

The authors have performed new experiments to address most of the concerns from the reviewers. I don't have additional comments.

Response: Thank you for reviewing our manuscript.

Reviewer #2 (Remarks to the Author):

The authors have addressed all of my concerns.

Response: Thanks for thoroughly reviewing our manuscript.

Reviewer #3 (Remarks to the Author):

Thank you for your effort in addressing my queries.

I do not have any more comments.

Response: We greatly appreciate the thorough review you provided for our study.

Reviewer #3 (Remarks on code availability):

I have examined the R script for SCENICR and RNAseq.

Response: Thank you for reviewing our scripts.

Reviewer #4 (Remarks to the Author):

The authors addressed all the points I raised.

Response: We greatly appreciate the thorough review and valuable suggestions you provided for our manuscript.

However, still some work as to be done concerning the reproducibility of the bioinformatics analysis. Please see below the review of the github

Reviewer #4 (Remarks on code availability):

Although the authors did a good work in the github repository. They must add in the readme a detailed indication where to retrieve the data used by each of the script.

The script https://github.com/XiaoXxin/Macrophage_Reparative/blob/main/CUTRUN BMDM STAT3/script_for_CUTRUN.R requires ./BMDM_STAT3.bigWig but the location where to retrieve such file is not indicated anywhere

Same problem apply to https://github.com/XiaoXxin/Macrophage_Reparative/blob/main/ChIPseq BMDM PPARg/script_for_ChIPseq.R which requires ./TA_summits.bed and ./WT_summits.bed

but from the github is not possible to identify where those files can be retrieved.
https://github.com/XiaoXxin/Macrophage_Reparative/blob/main/Lipidomics/script_for_lipidomics.R lacks the location of M2c_M0.all.txt
In https://github.com/XiaoXxin/Macrophage_Reparative/blob/main/scRNAseq SCENIC/sc_script_for_SCENIC.R
the path to download from https://resources.aertslab.org "mm9-500bp-upstream-7species.mc9nr.feather", "mm9-tss-centered-10kb-7species.mc9nr.feather" is not complete, it hust points to the main folder.
All scripts should be carefully revised to include the location of the input files. Additionally, the version of R and the R libraries used in each script must be provided.
Response: We have added detailed information to indicate the location of the input files in each R script and readme file. The version of R has been included in the readme file of our GitHub repository, and the version of R libraries used in this study have been provided in each script.